ACS APPLIED MATERIALS & INTERFACES

Research Article

www.acsami.org

Influence of Exciton Localization on the Emission and Ultraviolet Photoresponse of ZnO/ZnS Core–Shell Nanowires

Xuan Fang,[†] Zhipeng Wei,*[,†] Rui Chen,*[,‡] Jilong Tang,[†] Haifeng Zhao,[§] Ligong Zhang,[§] Dongxu Zhao,[§] Dan Fang,[†] Jinhua Li,[†] Fang Fang,[†] Xueying Chu,[†] and Xiaohua Wang[†]

[†]State Key Laboratory of High Power Semiconductor Lasers, School of Science, Changchun University of Science and Technology, 7089 Wei-Xing Road, Changchun 130022, People's Republic of China

[‡]Department of Electrical and Electronic Engineering, South University of Science and Technology of China, Shenzhen, Guangdong 518055, People's Republic of China

[§]Changchun Institute of Optics, Fine Mechanics and Physics, Chinese Academy of Science, Changchun 130033, People's Republic of China

ABSTRACT: The structural and optical properties of ZnO and ZnO/ZnS core–shell nanowires grown by a wet chemical method are investigated. The near-bandgap ultraviolet (UV) emission of the ZnO nanowires was enhanced by four times after coating with ZnS. The enhanced emission was attributed to surface passivation of the ZnO nanowires and localized states introduced during ZnS growth. The emission of the ZnO and ZnO/ZnS core–shell nanowires was attributed to neutral donor-bound excitons and localized excitons, respectively. Localized states prevented excitons from diffusing to nonradiative recombination centers, so therefore contributed to the enhanced emission. Emission from the localized exciton was not sensitive to temperature, so emission from the ZnO/ZnS core–shell nanowires was more stable at higher temperature. UV photodetectors based on the ZnO and ZnO/ZnS core–shell nanowires were fabricated. Under UV excitation, the device based on the ZnO/ZnS core–shell nanowires exhibited a photocurrent approximately 40 times higher than that of the device based on the ZnO nanowires. The differing photoresponse of the detectors was consistent with the existence of surface passivation and localized states. This study provides a means for modifying the optical properties of ZnO materials, and demonstrates the potential of ZnO/ZnS core–shell nanowires in UV excitonic emission and detection.

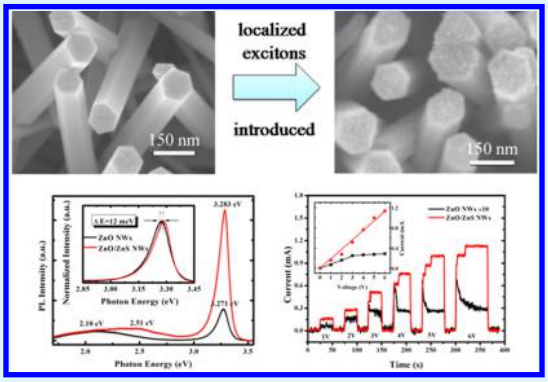

KEYWORDS: *core–shell structure, photoluminescence, exciton localization, surface passivation, photocurrent*

1. INTRODUCTION

One-dimensional (1D) nanostructures have received much attention in scientific investigation and potential application.[1−3] They can be used to fabricate nanoscale electronic, optoelectronic, and electrochemical devices.[4−10] ZnO is a semiconductor with a wide direct bandgap and large exciton binding energy and has been much studied in optoelectronics. ZnO 1D nanostructures exhibit favorable hardness and optical and piezoelectric properties, so they have potential in optically pumped nanolasers,[11] biosensors,[12] vertical nanowire field-effect transistors,[13] piezoelectric nanogenerators,[4,5,14] memory devices,[15] spintronics devices,[16] and photodetectors.[17−20]

The optoelectronic properties of nanomaterials are greatly influenced by their surface state, such as surface defects and dangling bonds.[21−23] These can cause defect emission and band bending, which lower the luminescence efficiency.[24,25] Surface states become more significant with increasing surface-to-volume ratio. Suppressing surface states while enhancing the ultraviolet (UV) emission of ZnO NWs will improve the performance of ZnO-based optoelectronic devices.

Various surface modification methods have been proposed, including plasma immersion ion implantation,[26] argon ion milling,[27] surface plasmon,[28] and surface passivation.[21] Heterogeneous coating using organic or inorganic materials (e.g., polymers and large-bandgap materials)[19,30] to construct core–shell structures is another surface modification approach.[29] Introducing localized states can prevent carrier migration toward nonradiative defects, which enhances optical efficiency.[31] Exploiting large-bandgap materials can enhance carrier absorption and emission intensity.[32,33] The broad available range of such materials promotes the fabrication of multifunctional materials, so heterogeneous coating is typically a more attractive approach.

ZnS is often used to modify ZnO surfaces, because of their similar physical properties.[19,20,34−36] ZnO/ZnS core–shell structures have received much recent attention for use in UV

Received: February 5, 2015
Accepted: April 28, 2015
Published: April 28, 2015

DOI: 10.1021/acsami.5b01100
ACS Appl. Mater. Interfaces 2015, 7, 10331−10336

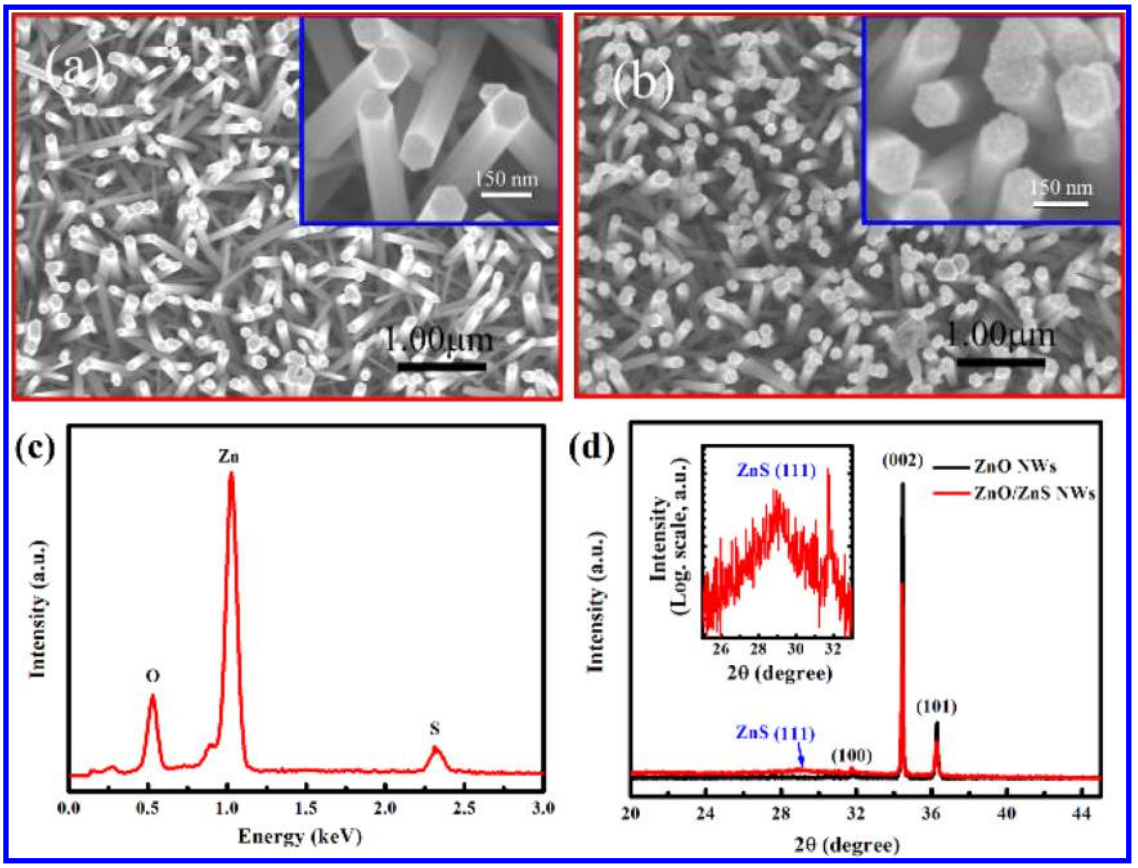

Figure 1. SEM images of (a) ZnO and (b) ZnO/ZnS core−shell nanowires, with insets showing higher magnification images; (c) EDS spectrum of ZnO/ZnS core−shell nanowires; (d) XRD patterns of ZnO and ZnO/ZnS core−shell nanowires.

detection. By efficient charge separation, ZnS can inject electrons into ZnO, which increases the photocurrent.[19,20] However, the mechanism for the enhanced (or decreased) UV emission by ZnO/ZnS remains unclear.[34−36] The device performance also requires improvement before it is suitable for practical application. In the current study, ZnO and ZnO/ZnS core−shell nanowires were synthesized, and their structural and optical properties have been investigated. Power- and temperature-dependent photoluminescence (PL) measurements indicated that UV emission of the ZnO and ZnO/ZnS core−shell nanowires resulted from neutral donor-bound excitons and localized excitons, respectively. Excitons' localization caused the enhanced photocurrent and photoresponse properties.

2. EXPERIMENTAL SECTION

ZnO nanowires were fabricated on quartz substrates using a ZnO seed film, which was deposited by atomic layer deposition (ALD) using a LabNano 9100 ALD system (Ensure Nanotech, Beijing, People's Republic of China). Growth conditions are available elsewhere.[37−39] To prepare ZnO/ZnS core−shell nanowires, the as-grown ZnO nanowires were immersed in 0.16 mol/L sodium sulfide (Na_2S) and zinc nitrate ($Zn(NO_3)_2$) solution for 2 h at 60 °C. The sample was then dried in air at 60 °C for 1 h.

Scanning electron microscopy (SEM) images and energy-dispersive X-ray (EDS) spectra were collected using a field-emission scanning electron microscope (Hitachi-4800, Tokyo, Japan) and attached EDS probe (GENE SIS 2000 XMS 60S, EDAX, Inc.), respectively, and were used to characterize sample morphologies and chemical compositions. X-ray diffraction (XRD) was used to characterize crystal structures. PL measurements were performed in conventional backscattering geometry, at 10−300 K in a closed-cycle He cryostat. The 325 nm line of a He−Cd laser was used as the excitation source. The laser power and beam size were 10 mW and 1 mm, respectively. For photoresponse measurements, 1 mm diamter In contacts were thermally welded on samples, at separation distances of 1 mm. The device was illuminated with the same laser beam under bias conditions, and a Keithley source meter (model 2400) was used to measure the photocurrent.

3. RESULTS AND DISCUSSION

Parts a and b of Figure 1 show SEM images of the ZnO and ZnO/ZnS core−shell nanowires, respectively. Figure 1a shows that the ZnO nanowires were vertically aligned on the substrate, with a well-defined hexagonal shape. The ZnO nanowire diameter was ∼100 nm. Figure 1b shows that the diameter of the ZnO/ZnS core−shell nanowires was larger because of the ZnS coating and that the nanowire surface became more roughened. Figure 1c shows the EDS spectrum of the ZnO/ZnS core−shell nanowires, in which Zn, O, and S were detected. The inset of Figure 1d shows the ZnS (111) diffraction peak of the XRD pattern of the ZnO/ZnS core−shell nanowires. Diffraction peaks characteristic of ZnO, such as ZnO (100), (002), and (101), were still observed after coating with ZnS. Sharp (002) diffraction peaks dominated the XRD patterns of both samples, indicating very high crystallinity and ZnO orientation along the crystallographic *c*-axis. These results confirmed that ZnO/ZnS core−shell nanowires were synthesized by the wet chemical method.

Figure 2 shows the room-temperature PL spectra of the samples. That of the ZnO nanowires exhibited two emission bands: a deep-level emission (DLE) at ∼2.10 eV, and a near-band-edge emission (NBE) at 3.271 eV. The orange DLE was

DOI: 10.1021/acsami.5b01100
ACS Appl. Mater. Interfaces 2015, 7, 10331−10336

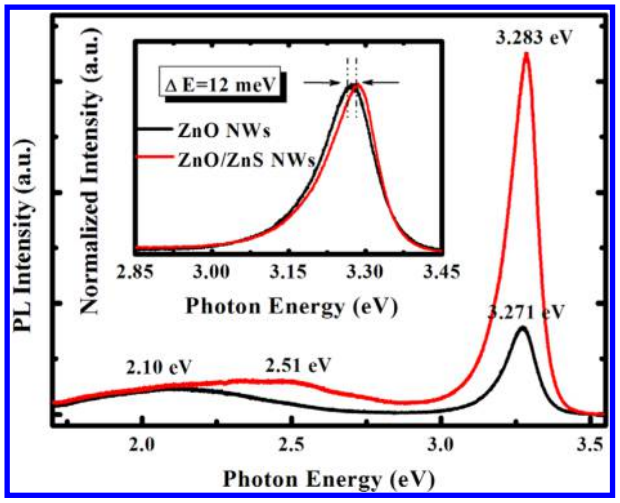

Figure 2. Room-temperature PL spectra of ZnO and ZnO/ZnS core–shell nanowires. Inset shows normalized UV emission.

ascribed to oxygen or water molecules on the nanowire surface.[19] The DLE emission of the ZnO/ZnS nanowires was broader, and the PL spectrum contained an additional peak at 2.51 eV, which may have been caused by ZnS defect emission.[19] The optical properties of the ZnO nanowires changed significantly after coating with ZnS. Holes in the ZnO core should theoretically by depleted because of type-II band alignment in the ZnO/ZnS core–shell nanowires, so charge separation should quench UV emission.[34] However, Figure 2 shows that the UV emission of the ZnO/ZnS core–shell nanowires was ∼4 times more intense than that of the ZnO nanowires. The UV emission peak of the ZnO/ZnS core–shell nanowires should also theoretically red-shift, compared with that of the ZnO nanowires,[34] but a blue-shift of ∼12 meV was observed, as shown in the inset of Figure 2. Similar reported observations were ascribed to the Burstein–Moss effect,[40] but this could not account for the current observations (will be discussed later).

Low-temperature and temperature-dependent PL measurements were carried out, to investigate the mechanism of the enhanced and blue-shifted UV emission. Figure 3a shows the PL emission of the ZnO and ZnO/ZnS core–shell nanowires at 10 K. For the ZnO nanowires, the emission peak at 3.352 eV was attributed to radiative recombination from neutral donor-bound excitons (D^0X) according to previous reports.[31,41] For the ZnO/ZnS core–shell nanowires, the emission peak at ∼3.354 eV showed no obvious shift, but an enhancement in intensity, and was also attributed to exciton transition. Peaks at 3.3 and 3.23 eV for the two samples were assigned to FX-1LO and FX-2LO, respectively.[27,42] The peak at 2.98 eV was assigned to Zn_i.[43] Power-dependent PL spectra are shown in Figure 3b. Increasing the excitation power from 0.1 to 10 mW resulted in an approximately linear increase in PL intensity. For the ZnO/ZnS core–shell nanowires, the emission peak red-shifted at higher laser power, which could have been caused by laser heating effect.[44] The integrated PL emission intensity at different excitation powers is shown in the inset of Figure 3b, and their relationship was of the form $I_{PL} \propto I_{EX}^{\alpha}$; I_{EX} is the power of the excitation laser radiation, and α represents the radiative recombination mechanism. For excitonic recombination, we have $1 < \alpha < 2$; for bandgap emission, $\alpha \approx 2$; if α is less than 1, it means a transition is related to impurity.[31,44,45] The inset of Figure 3b shows that the integrated PL intensity of the two samples exhibited a power-law dependence with excitation density. Fitting the experimental data yielded a α of 0.88 for the ZnO nanowires, which indicated their UV emission was of bond-exciton-related emission (D^0X),[44] similarly to previous results.[31] A α of 0.91 was obtained for the ZnO/ZnS core–shell nanowires; the differing α values of the two samples indicated that the bond exciton of the ZnO/ZnS nanowires was not D^0X, but this emission can be ascribed to the excitonic recombination. Here we deduced that this emission was caused by localized states introduced by the ZnS coating.[44,45]

Figure 4 shows the temperature-dependent PL spectra of the ZnO and ZnO/ZnS core–shell nanowires. No free exciton emission was observed for either sample. At room temperature, the emission of ZnO was dominated by D^0X and the emission of ZnO/ZnS by localized excitons. Parts a and b of Figure 5 show the emission peak position and intensity of the samples, respectively, with increasing temperature. The photon energy of D^0X of the ZnO nanowires decreased with increasing temperature. This indicated that this emission was more sensitive to temperature and could be fitted using the empirical Varshni equation.[46,47] The emission intensity also decreased with increasing temperature, but the emission position of the ZnO/ZnS core–shell nanowires remained higher than that of the ZnO nanowires, even at room temperature. In addition, the

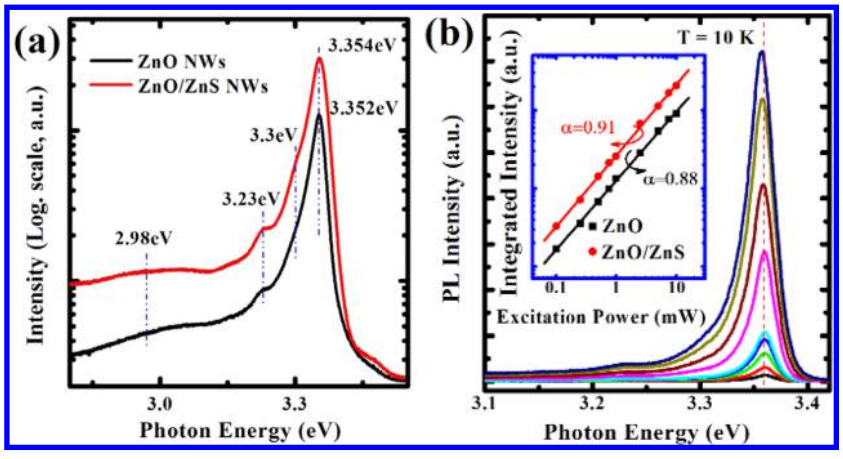

Figure 3. (a) Low-temperature (10 K) PL spectra of ZnO and ZnO/ZnS core–shell nanowires; (b) power-dependent PL spectra of ZnO/ZnS core–shell nanowires. Inset shows relationship between integrated PL intensity and laser excitation power.

DOI: 10.1021/acsami.5b01100
ACS Appl. Mater. Interfaces 2015, 7, 10331–10336

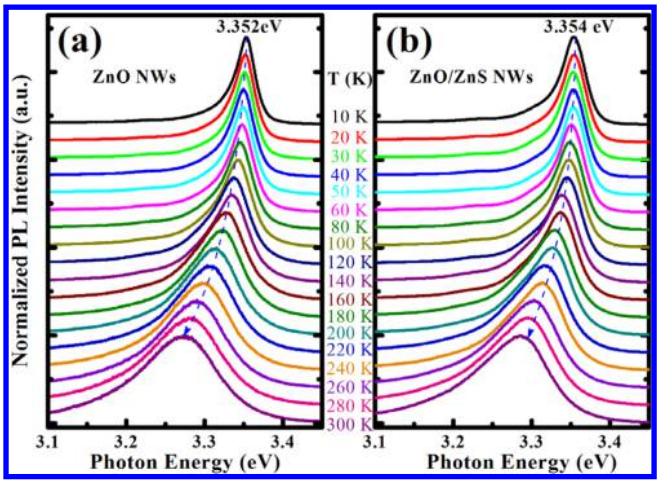

Figure 4. Temperature-dependent PL spectra of (a) ZnO and (b) ZnO/ZnS core−shell nanowires.

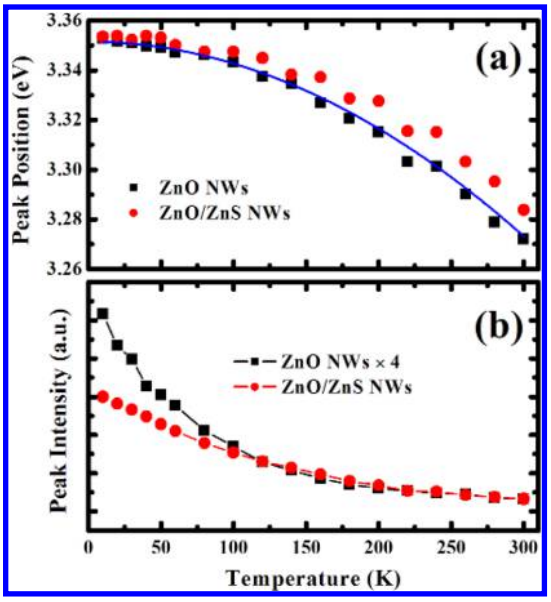

Figure 5. Emission (a) photon energy and (b) peak intensity of ZnO and ZnO/ZnS core−shell nanowires with increasing temperature.

photon energy of the emission from ZnO/ZnS with temperature cannot be fitted by the empirical Varshni equation,[46,47] which implied that it is not from D^0X again. The relationship between emission intensity and temperature in Figure 5b shows that the ZnO emission decreased by 16 times with increasing temperature from 10 to 300 K, whereas the ZnO/ZnS emission decreased by only 9 times. Thus, the emission of the ZnO/ZnS core−shell nanowires was more stable than that of the ZnO nanowires. At higher temperature, the excitons of ZnO/ZnS would be free and enhance the UV emission, which means these excitons were bounded by a much deeper energy level. And localized excitons are reportedly insensitive to temperature, so the emission at ∼3.354 eV can be assigned to exciton localization. These localized states in ZnO/ZnS prevented excitons (generated from ZnO nanowires) from being trapped by defect states, so they were responsible for the UV emission enhancement and blue-shift at room temperature.

The core−shell structure greatly improved the luminescent properties of the ZnO. ZnO/ZnS core−shell nanowires were then exploited in nano-optoelectronic devices. A photodetector was fabricated using the ZnO/ZnS core−shell nanowires, as shown by the schematic in Figure 6. The photocurrent was

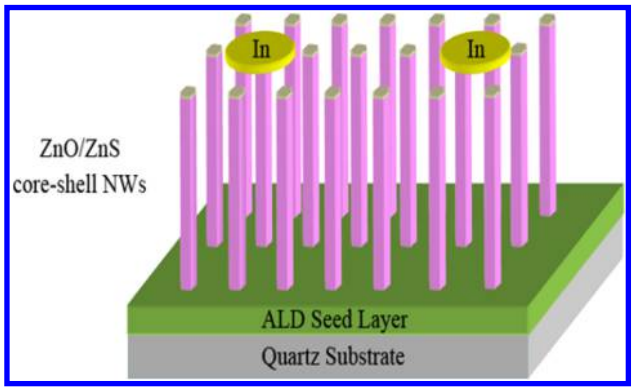

Figure 6. Schematic of the device containing ZnO/ZnS core−shell nanowires.

measured by switching the UV illumination at 325 nm on and off, for 100 s each cycle. The time-dependent photocurrents of the ZnO- and ZnO/ZnS-based devices are shown in Figure 7a.

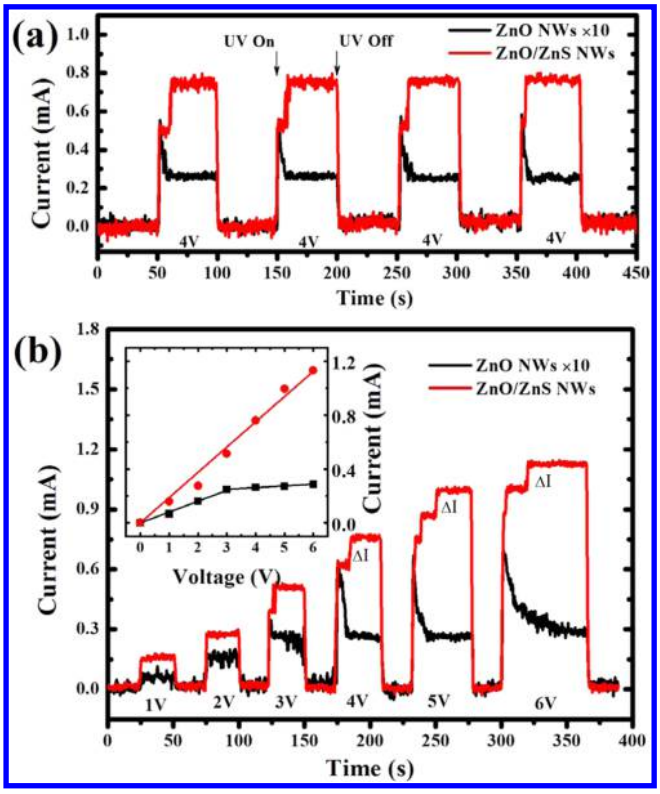

Figure 7. (a) Photocurrents of ZnO and ZnO/ZnS core−shell nanowires at 4 V; (b) photocurrents of ZnO and ZnO/ZnS core−shell nanowires at different biases.

Under a 4 V bias, both devices exhibited reproducible photoresponse behavior. The photocurrent of the ZnO-based device increased quickly upon illumination and then gradually decreased, a few seconds later reaching a stable value of ∼0.021 mA. This was explained by the heating effect or surface-related absorption (O_2), as previously discussed in detail.[19,48] For the ZnO/ZnS-based device, UV illumination did not result in a time decay in the photocurrent. The ZnO/ZnS-based device exhibited a photocurrent of ∼0.796 mA, which was ∼40 times

DOI: 10.1021/acsami.5b01100
ACS Appl. Mater. Interfaces 2015, 7, 10331−10336

that of the ZnO-based device.[34] The photocurrent contained two components, one of which was attributed to the ZnO photoresponse. The ZnO surface was covered by a ZnS layer which suppressed surface absorption processes, so the device exhibited a stable photocurrent in the first few seconds. Another higher photocurrent was then observed. The conduction and valence bands in the ZnO/ZnS type-II heterostructure are at higher energies than in ZnO, so photogenerated carriers can potentially transfer from ZnS to ZnO, thus decreasing the PL intensity.[34,49] However, the room-temperature PL results in Figure 2 showed an enhanced PL intensity for the ZnO/ZnS core−shell nanowires. This enhanced photocurrent was thought to be related to exciton localization from ZnS, but not to electrons transferred from ZnS to ZnO. To investigate this hypothesis, Figure 7b shows photocurrents recorded at different biases. At a bias of <3 V, only photocurrent from ZnO was detected. At sufficiently large bias, a change in current (ΔI) of 0.13 mA was apparent, and the response time increased. It is interesting to note that the photocurrent difference, ΔI, remained the same, which implied that the energy barrier (from ZnO/ZnS type-II heterostructure interface) that confines the exciton was the same. Thus, when the bias was high enough to shift the band and activate the localized exciton in ZnO/ZnS nanowires, we can observe it. So ΔI was the photocurrent from localized states. This showed that localized excitons required a certain amount of energy to become free, which increased the response time. This was also consistent with the magnified photocurrent being related to exciton localization from ZnS. At a bias of >4 V, the photocurrent of the ZnO-based device gradually saturated. The Figure 7b inset shows that the ZnO/ZnS-based device exhibited a linear relationship between photocurrent and bias. Coating with ZnS greatly improved the photoresponse of the ZnO-based device.

4. CONCLUSIONS

ZnO/ZnS core−shell nanowires of high crystallinity and orientation along the crystallographic *c*-axis were prepared. The ZnO/ZnS core−shell nanowires exhibited enhanced UV emission, compared with the ZnO core−shell nanowires. Power- and temperature-dependent PL spectra were analyzed, which indicated that the origin of this was localized excitons introduced by the ZnS coating. The ZnS shell also resulted in green emission by the ZnO/ZnS core−shell nanowires. The ZnS shell suppressed surface states in the ZnO nanowires and prevented exciton diffusion to nonradiative recombination centers of ZnO, which enhanced the UV emission. The photoresponse of devices based on the core−shell nanowires was improved by the ZnS passivation effect and localized excitons. The device based on the ZnO/ZnS core−shell nanowires exhibited a much higher photocurrent than that based on the ZnO core−shell nanowires. Thus, localized excitons are important for the optical properties and performance of such devices.

AUTHOR INFORMATION

Corresponding Authors

*(Z.W.) E-mail: zpweicust@126.com.
*(R.C.) E-mail: chen.r@sustc.edu.cn.

Notes

The authors declare no competing financial interest.

ACKNOWLEDGMENTS

This research was supported by the National Natural Science Foundation of China (Grant Nos. 61204065, 61205193, 61307045, 61404009, 61474010, 11404219, and 11404161), the Developing Project of Science and Technology of Jilin Province (Grant No. 20130101026JC), and the National Key Laboratory of High Power Semiconductor Lasers Foundation (Grant Nos. 9140C3101011120C031115, 9140C310104110C3101, 9140C310102130C31107, 9140C3101024C310004, and 9140C310101120C031115). R.C. acknowledges the startup fund from SUSTC and the National 1000 Plan for Young Talents.

REFERENCES

(1) Chu, S.; Wang, G. P.; Zhou, W. H.; Lin, Y. Q.; Chernyak, L.; Zhao, J. Z.; Kong, J. Y.; Li, L.; Ren, J. J.; Liu, J. L. Electrically Pumped Waveguide Lasing From ZnO Nanowires. *Nat. Nanotechnol.* **2010**, *6*, 506−510.

(2) Zhou, S. Y.; Chu, X. Y.; Li, J. H.; Fang, F.; Fang, X.; Wei, Z. P.; Chen, F.; Wang, X. H. Enhanced Mn^{2+} Emission in ZnS:Mn Nanoparticles by Surface Plasmon Resonance of Gold Nanoparticles. *J. Appl. Phys.* **2014**, *116*, No. 014306.

(3) Yan, J. F.; Zhou, F. TiO_2 Nanotubes: Structure Optimization for Solar Cells. *J. Mater. Chem.* **2011**, *21*, 9406−9418.

(4) Wang, S. H.; Lin, L.; Wang, Z. L. Nanoscale Triboelectric-Effect-Enabled Energy Conversion for Sustainably Powering Portable Electronics. *Nano Lett.* **2012**, *12*, 6339−6346.

(5) Lee, S.; Bae, S. H.; Lin, L.; Yang, Y.; Park, C.; Kim, S. W.; Cha, S. N.; Kim, H.; Park, Y. J.; Wang, Z. L. Super-Flexible Nanogenerator for Energy Harvesting from Gentle Wind and as an Active Deformation Sensor. *Adv. Funct. Mater.* **2013**, *23*, 2445−2449.

(6) Eunice, S. P. L.; Siu, F. Y. UV Random Lasing Action in p-SiC(4H)/i-ZnO−SiO_2 Nanocomposite/n-ZnO:Al Heterojunction Diodes. *Adv. Mater.* **2006**, *18*, 1685−1688.

(7) Zhu, H.; Shan, C. X.; Zhang, J. Y.; Zhang, Z. Z.; Li, B. H.; Zhao, D. X.; Yao, B.; Shen, D. Z.; Fan, X. W.; Tang, Z. K.; Hou, X. H.; Choy, K. L. Low-Threshold Electrically Pumped Random Lasers. *Adv. Mater.* **2010**, *22*, 1−5.

(8) Guo, Z.; Li, H. W.; Zhou, L. Q.; Zhao, D. X.; Wu, Y. H.; Zhang, Z. Q.; Zhang, W.; Li, C. Y.; Yao, J. Large-Scale Horizontally Aligned ZnO Microrod Arrays with Controlled Orientation, Periodic Distribution as Building Blocks for Chip-in Piezo-Phototronic LEDs. *Small* **2015**, *11*, 438−445.

(9) Lupan, O.; Pauporté, T.; Viana, B. Low-Voltage UV-Electroluminescence from ZnO-Nanowire Array/p-GaN Light-Emitting Diodes. *Adv. Mater.* **2010**, *22*, 3298−3302.

(10) Xing, G. Z.; Wang, D. D.; Cheng, C. J.; He, M.; Li, S.; Wu, T. Emergent Ferromagnetism in ZnO/Al_2O_3 Core-Shell Nanowires: Towards Oxide Spinterfaces. *Appl. Phys. Lett.* **2013**, *103*, No. 022402.

(11) Huang, M. H.; Mao, S.; Feick, H.; Yan, H. Q.; Wu, Y. Y.; Kind, H.; Weber, E.; Russo, R.; Yang, P. D. Room-Temperature Ultraviolet Nanowire Nanolasers. *Science* **2001**, *292*, 1897−1899.

(12) Liu, T. Y.; Liao, H. C.; Lin, C. C.; Hu, S. H.; Chen, S. Y. Biofunctional ZnO Nanorod Arrays Grown on Flexible Substrates. *Langmuir* **2006**, *22*, 5804−5809.

(13) Ng, H. T.; Han, J.; Yamada, T.; Nguyen, P.; Chen, Y. P.; Meyyappan, M. Single Crystal Nanowire Vertical Surround-Gate Field-Effect Transistor. *Nano Lett.* **2004**, *4*, 1247−1252.

(14) Wang, Z. L.; Song, J. Piezoelectric Nanogenerators Based on Zinc Oxide Nanowire Arrays. *Science* **2006**, *312*, 242−246.

(15) Bera, A.; Peng, H. Y.; Lourembam, J.; Shen, Y.; Sun, X. W.; Wu, T. A Versatile Light-Switchable Nanorod Memory: Wurtzite ZnO on Perovskite $SrTiO_3$. *Adv. Funct. Mater.* **2013**, *23*, 4977−4984.

(16) Tian, Y. F.; Bakaul, S. R.; Wu, T. Oxide Nanowires for Spintronics: Materials and Devices. *Nanoscale* **2012**, *4*, 1529−1540.

(17) Guo, L.; Zhang, H.; Zhao, D. X.; Yao, B.; Li, B. H.; Zhang, Z. Z.; Shen, D. Z. The Growth and the Ultraviolet Photoresponse Properties

DOI: 10.1021/acsami.5b01100
ACS Appl. Mater. Interfaces 2015, 7, 10331−10336

of the Horizontal Growth ZnO Nanorods. *Mater. Lett.* **2011**, *65*, 1495−1498.
(18) Sun, K.; Jing, Y.; Park, N.; Li, C.; Bando, Y.; Wang, D. L. Solution Synthesis of Large-Scale, High-Sensitivity ZnO/Si Hierarchical Nanoheterostructure Photodetectors. *J. Am. Chem. Soc.* **2010**, *132*, 15465−154679.
(19) Bera, A.; Basak, D. Photoluminescence and Photoconductivity of ZnS-Coated ZnO Nanowires. *ACS Appl. Mater. Interfaces* **2010**, *2*, 408−412.
(20) Shuai, X. M.; Shen, W. Z. A Facile Chemical Conversion Synthesis of ZnO/ZnS Core/Shell Nanorods and Diverse Metal Sulfide Nanotubes. *J. Phys. Chem. C* **2011**, *115*, 6415−6422.
(21) Wang, B.; Wei, Z. P.; Li, M.; Liu, G. J.; Zou, Y. G.; Xing, G. Z.; Tan, T. T.; Li, S.; Chu, X. Y.; Fang, F.; Fang, X.; Li, J. H.; Wang, X. H.; Ma, X. H. Tailoring the Photoluminescence Characteristics of p-Type GaSb: The Role of Surface Chemical Passivation. *Chem. Phys. Lett.* **2013**, *556*, 182−187.
(22) Guo, Y. Z.; Lin, L.; Robertson, J. Nitrogen Passivation at GaAs:Al_2O_3 Interfaces. *Appl. Phys. Lett.* **2013**, *102*, No. 091606.
(23) Regulacio, M. D.; Win, K. Y.; Lo, S. L.; Zhang, S. Y.; Zhang, X. H.; Wang, S.; Han, M. Y.; Zheng, Y. G. Aqueous Synthesis of Highly Luminescent $AgInS_2$−ZnS Quantum Dots and Their Biological Applications. *Nanoscale* **2013**, *5*, 2322−2327.
(24) Geppert, I.; Eizenberg, M.; Ali, A.; Datta, S. Band Offsets Determination and Interfacial Chemical Properties of the Al_2O_3/GaSb System. *Appl. Phys. Lett.* **2010**, *97*, No. 162109.
(25) Leung, Y. H.; Chen, X. Y.; Ng, A. M. C.; Guo, M. Y.; Liu, F. Z.; Djurisic, A. B.; Chan, W. K.; Shi, X. Q.; Hove, M. A. V. Green Emission in ZnO Nanostructures-Examination of the Roles of Oxygen and Zinc Vacancies. *Appl. Surf. Sci.* **2013**, *271*, 202−209.
(26) Yang, Y.; Sun, X. W.; Tay, B. K.; Cao, P. H. T.; Wang, J. X.; Zhang, X. H. Revealing the Surface Origin of Green Band Emission from ZnO Nanostructures by Plasma Immersion Ion Implantation Induced Quenching. *J. Appl. Phys.* **2008**, *103*, No. 064307.
(27) Chen, R.; Ye, Q. L.; He, T. C.; Wu, T.; Sun, H. D. Uniaxial Tensile Strain and Exciton−Phonon Coupling in Bent ZnO Nanowires. *Appl. Phys. Lett.* **2011**, *98*, No. 241916.
(28) Shao, D.; Sun, H.; Yu, M.; Lian, J.; Sawyer, S. Enhanced Ultraviolet Emission from Poly(vinyl alcohol) ZnO Nanoparticles Using a SiO_2−Au Core/Shell Structure. *Nano Lett.* **2012**, *12*, 5840−5844.
(29) Zhang, J. T.; Tang, Y.; Lee, K.; Ouyang, M. Nonepitaxial Growth of Hybrid Core-Shell Nanostructures with Large Lattice Mismatches. *Science* **2010**, *327*, 1634−1638.
(30) Liu, K. W.; Chen, R.; Xing, G. Z.; Wu, T.; Sun, H. D. Photoluminescence Characteristics of High Quality ZnO Nanowires and its Enhancement by Polymer Covering. *Appl. Phys. Lett.* **2010**, *96*, No. 023111.
(31) Chen, R.; Ye, Q. L.; He, T. C.; Ta, V. D.; Ying, Y. J.; Tay, Y. Y.; Wu, T.; Sun, H. D. Exciton Localization and Optical Properties Improvement in Nanocrystal-Embedded ZnO Core−Shell Nanowires. *Nano Lett.* **2013**, *13*, 734−739.
(32) Grinblat, G.; Gonzalez, L. J. B.; Nunes, L. A. O.; Tirado, M.; Comedi, D. Enhanced Optical Properties and (Zn, Mg) Interdiffusion in Vapour Transport Grown ZnO/MgO Core/shell Nanowires. *Nanotechnology* **2014**, *25*, No. 035705.
(33) Meng, X. Q.; Peng, H. W.; Gai, Y. Q.; Li, J. B. Influence of ZnS and MgO Shell on the Photoluminescence Properties of ZnO Core/Shell Nanowires. *J. Phys. Chem. C* **2010**, *114*, 1467−1471.
(34) Wang, K.; Chen, J. J.; Zeng, Z. M.; Tarr, J.; Zhou, W. L. Synthesis and Photovoltaic Effect of Vertically Aligned ZnO/ZnS Core/Shell Nanowire Arrays. *Appl. Phys. Lett.* **2010**, *96*, No. 123105.
(35) Panigrahi, S.; Sarkar, S.; Basak, D. Metal-Free Doping Process to Enhance the Conductivity of Zinc Oxide Nanorods Retaining the Transparency. *ACS Appl. Mater. Interfaces* **2012**, *4*, 2709−2716.
(36) Li, J. H.; Zhao, D. X.; Meng, X. Q.; Zhang, Z. Z.; Zhang, J. Y.; Shen, D. Z.; Lu, Y. M.; Fan, X. W. Enhanced Ultraviolet Emission from ZnS-Coated ZnO Nanowires Fabricated by Self-Assembling Method. *J. Phys. Chem. B* **2006**, *110*, 14685−14687.
(37) Fang, X.; Li, J. H.; Zhao, D. X.; Shen, D. Z.; Li, B. H.; Wang, X. H. Phosphorus-Doped p-Type ZnO Nanorods and ZnO Nanorod p-n Homojunction LED Fabricated by Hydrothermal Method. *J. Phys. Chem. C* **2009**, *113*, 21208−21212.
(38) Fang, X.; Wang, X. H.; Zhao, D. X.; Zhao, H. F.; Fang, F.; Wei, Z. P.; Li, J. H.; Chu, X. Y.; Wang, F.; Wang, D. D.; Yan, Y. S. Electroluminescence of ZnO Nanorods/ZnMgO Films/p-SiC Structure Heterojunction LED. *Phys. E (Amsterdam, Neth.)* **2014**, *59*, 93−97.
(39) Guo, Z.; Zhao, D. X.; Liu, Y. C.; Shen, D. Z.; Yao, Bin.; Zhang, Z. Z.; Li, B. H. Electrically Pumped Single-Mode Lasing Emission of Self-Assembled n-ZnO Microcrystalline Film/p-GaN Heterojunction Diode. *J. Phys. Chem. C* **2010**, *114*, 15499−15503.
(40) Panda, S. K.; Dev, A.; Chaudhuri, S. Fabrication and Luminescent Properties of *c*-Axis Oriented ZnO−ZnS Core−Shell and ZnS Nanorod Arrays by Sulfidation of Aligned ZnO Nanorod Arrays. *J. Phys. Chem. C* **2007**, *111*, 5039−5043.
(41) Lima, S. A. M.; Sigoli, F. A.; M, J., Jr.; Davolos, M. R. Luminescent Properties and Lattice Defects Correlation on Zinc Oxide. *Int. J. Inorg. Mater.* **2001**, *3*, 749−754.
(42) Fang, F.; Zhao, D. X.; Li, B. H.; Zhang, Z. Z.; Shen, D. Z.; Wang, X. H. Bending-Induced Enhancement of Longitudinal Optical Phonon Scattering in ZnO Nanowires. *J. Phys. Chem. C* **2010**, *114*, 12477−12480.
(43) Lin, B. X.; Fu, Z. X. Green Luminescent Center in Undoped Zinc Oxide Films Deposited on Silicon Substrates. *Appl. Phys. Lett.* **2001**, *79*, No. 943.
(44) Bergman, L.; Chen, X. B.; Morrison, J. L.; Huso, J.; Purdy, A. P. Photoluminescence Dynamics in Ensembles of Wide-Band-Gap Nanocrystallites and Powders. *J. Appl. Phys.* **2004**, *96*, 675−682.
(45) Satake, A.; Masumoto, Y. Localized Exciton and its Stimulated Emission in Surface Mode from Single-layer $In_xGa_{1-x}N$. *Phys. Rev. B* **1998**, *57*, R2041−R2044.
(46) Chen, R.; Li, D. H.; Liu, B.; Peng, Z. P.; Gurzadyan, G. G.; Xiong, Q. H.; Sun, H. D. Optical and Excitonic Properties of Crystalline ZnS Nanowires: Toward Efficient Ultraviolet Emission at Room Temperature. *Nano Lett.* **2010**, *10*, 4956−4961.
(47) Varshni, Y. P. Temperature Dependence of the Energy Gap in Semiconductor. *Physica* **1967**, *34*, 149−154.
(48) Bera, A.; Basak, D. Role of Defects in the Anomalous Photoconductivity in ZnO Nanowires. *Appl. Phys. Lett.* **2009**, *94*, No. 163119.
(49) Dabbousi, B. O.; Viejo, J. R.; Mikulec, F. V.; Heine, J. R.; Mattoussi, H.; Ober, R.; Jensen, K. F.; Bawendi, M. G. (CdSe)ZnS Core-Shell Quantum Dots: Synthesis and Characterization of a Size Series of Highly Luminescent Nanocrystallites. *J. Phys. Chem. B* **1997**, *101*, 9463−9475.

DOI: 10.1021/acsami.5b01100
ACS Appl. Mater. Interfaces 2015, 7, 10331−10336